

UV-Laser Marking of a TiO₂-Containing ABS Material

M.J. Clemente,¹ C. Lavieja,² J.I. Peña,² L. Oriol ¹

¹Instituto de Ciencia de Materiales de Aragón (ICMA), Universidad de Zaragoza-CSIC, Dpto. Química Orgánica, Facultad de Ciencias, Pedro Cerbuna 12, Zaragoza 50009, España

²Instituto de Ciencia de Materiales de Aragón (ICMA), Universidad de Zaragoza-CSIC, Dpto. Ciencia y Tecnología de Materiales y Fluidos, EINA, María de Luna 3, Zaragoza 50018, España

Marking of titanium dioxide-containing ABS polymeric samples was accomplished using a UV laser that induces a white to grey color change with only a minor alteration of the plastic material. The characterization of this marking process has been conducted by different techniques to determine the quality of the UV-laser marking and to gain an insight into how the plastic material is affected by laser irradiation. Surface characterization was performed and tests were conducted to evaluate the potential applications of this UV-marking process. POLYM. ENG. SCI., 00:000–000, 2017. © 2017 Society of Plastics Engineers

INTRODUCTION

The applications of laser technology usually involve processes such as welding or cutting, mostly on metals, surface treatments such as drilling or marking surfaces, mainly on plastics, and curing of paints and inks. Processing with lasers takes advantage of the characteristics of laser light, in particular, the high energy density and directionality achieved with lasers allows strongly localized heat- or photo-treatment of materials with a spatial resolution better than 100 nm [1]. Furthermore, laser technology offers different advantages as it is a noncontact process that is compatible with computer numerical control with a high flexibility. However, the disadvantages of this approach, e.g., the high costs and possible material damage, should be considered.

In reference to marking processes are concerned, lasers are particularly useful because they can be safely integrated into assembly lines, applied to products with various geometries and be controlled by a computer, thus resulting in high reproducibility, high speed, and high throughput. This technology provides rapid customization in mass production. In addition, laser marking avoids the use of inks and pretreatment of the surface material. Applications range from product recognition and identification to the printing of alphanumeric characters, symbols, and logos [2].

The legibility characteristics of a mark, such as contrast and minimum width, depend on the material properties, e.g., absorptivity, as well as on the laser marking parameters: power density, focal position, and marking speed. CO₂, Nd:YAG and excimer lasers are the three most widely available commercial lasers used for industrial laser-marking applications [3]. Laser irradiation can give rise to different effects in plastic materials,

such as engraving, ablation, foaming, carbonization, photoreduction, bleaching, and color formation [4]. Most of the previous studies performed on polymers were conducted using excimer laser sources [5–14]. It has been reported that thermal effects and photochemical reactions coexist during ablation [15, 16] and, on operating with laser fluences below the material ablation threshold, the original polymer surface is modified by UV photons [17, 18], which result in photolytic modification and activation [19].

ABS (acrylonitrile–butadiene–styrene) is a thermoplastic copolymer with a high impact resistance and toughness. This polymer is widely used to produce home appliances amongst other applications. Furthermore, it is a material of interest to study the enhancement of aesthetical markings involving a change in color, for instance from a white pigmented polymeric material to a grey color in the selected polymer matrix [20]. The majority of resins, including polyolefins and styrenic polymers, are not easy to mark using laser technology. Plastics with a low absorption level of laser light show practically no reaction to laser irradiation. The incorporation of pigments makes the plastic receptive to laser light and, as a consequence, high contrast and visible marks can be achieved at relatively low laser intensity in the range of IR wavelengths [21]; however, the quality of the marks is not sufficient for aesthetical applications. A widely used additive is the TiO₂ that is primarily employed as a whitener in polymers [22] because to its light scattering properties and good thermal and chemical stability. This molecule absorbs UV-radiation [23] and it has been described as a powerful photocatalyst [24].

In the present study, a frequency-tripled Nd:YAG laser emitting at 355 nm (UV laser) was selected to produce aesthetical marks on white ABS. Different superficial analyses were conducted to describe the characteristics of the affected surface, including the microstructure, roughness and color to characterize the quality of the mark. Furthermore, the way in which the chemical structure of the polymer is affected by the UV-laser marking was investigated. For this purpose, several spectroscopic and microscopic techniques were employed. Finally, preliminary quality tests were performed to analyze the resistance of the marks to climatic conditions and common chemicals.

EXPERIMENTAL

The laser used in this work was the Powerline E20 UV commercialized by Rofin. This laser system operates at a wavelength of 355 nm in the nanosecond pulsewidth range. The pulse work energy of the laser is 125 μJ. In this study, 1 cm × 1 cm square areas were marked using galvanometric mirrors that were large enough to perform the superficial and chemical characterization. The number of spots per area (*N*) or dots per inch (DPI) is a function of the pulse frequency, the scanning speed and the hatch, i.e., the distance between consecutive

Additional Supporting Information may be found in the online version of this article.

Correspondence to: M.J. Clemente; e-mail: mjcleme@unizar.es or L. Oriol; e-mail: loriol@unizar.es

Contract grant sponsor: Seventh Framework Programme of the European Union under the UV-MARKING project; contract grant number: 314630.

DOI 10.1002/pen.24749

Published online in Wiley Online Library (wileyonlinelibrary.com).

© 2017 Society of Plastics Engineers

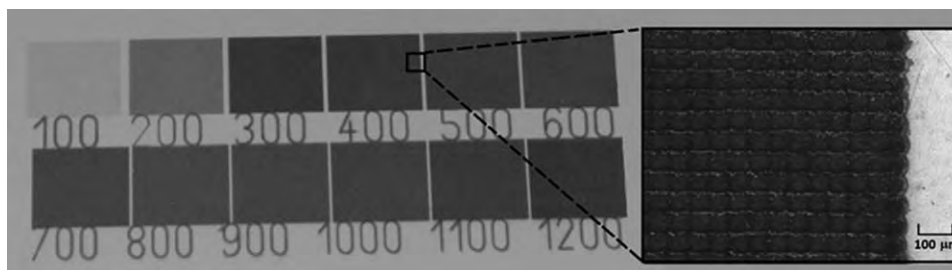


FIG. 1. Different marks made with the UV-laser in the ABS sample at different DPI ranging from 100 to 1,200. Right: Detail of the sample marked at 400 DPI.

tracks made by the laser scanning, according to Eq. 1. Therefore, differences in the appearance of marks can be achieved through variations in the number of DPI by simply modifying the other parameters while keeping the pulse frequency constant, see Supporting Information Figure SI.1.

$$N = \frac{\text{number of spots}}{\text{cm}^2} = \frac{\text{freq}}{\text{speed}_{\text{scan}} \times \text{hatch}} = \frac{\text{DPI}_x \times \text{DPI}_y}{6.4516} \quad (1)$$

The total energy deposited on the surface (E_t) was calculated by multiplying the laser energy per pulse (E_p) by the number of spots (N). So, the DPI number is directly correlated to the total energy deposited on the surface.

Injected discs of titanium dioxide-containing ABS from Elix Polymers (reference number: P2H-AT LNS 202) were used for laser marking. The color changes were measured using a Konica Minolta spectrophotometer and SCI (specular component included) values are reported. The spot diameter for measurements was 6 mm. Optical confocal microscopy was conducted using a Nikon Sensofar Plμ2300 system. Environmental scanning electron microscopy (ESEM) measurements were performed using a QUANTA FEG 250 system. The sample was directly observed without coating. Attenuated total reflectance-infrared spectroscopy (ATR-FTIR) was performed using a Vertex 70 Bruker FTIR spectrophotometer equipped with a GoldenGate Specac ATR accessory. Thermogravimetric analysis (TGA) was performed on a TGA Q5000IR system from TA Instruments at a rate of 10°C/min under an air atmosphere up to 750°C. Inductively coupled plasma optical emission spectroscopy (ICP-OES) to determine the percentage of titanium dioxide was performed on an IRIS ADVANTAGE system from Thermo Jarrel Ash. ABS pellets were first calcinated at 500°C for 5 h before ICP-OES analysis. X-ray Photoelectron Spectroscopy (XPS) measurements were performed on a Kratos AXIS ultra DLD (Mono Al Ka, Power: 120 W (10mA, 15kV).

Scratch tests were performed with an Erichsen pen having a linear movement. After the tests, the scratch width was measured by confocal microscopy and compared with the scratch in unmarked material and pad printing samples used as a reference (pad printing is widely used in the decoration of plastic materials). The force in this device can be changed from 2 to 10 N. The scratch speed was 28 mm/s. Climate tests were conducted on five samples in an ATLAS SUNTEST XXL+ climate chamber with a Xenon Lamp. The standard method applied was UNE-EN ISO 4892 standard and this involved a cycle of 102 min irradiation at $65 \pm 3^\circ\text{C}$, $20 \pm 10\%$ humidity and 0.51 ± 0.02

W ($\text{m}^2 \text{ nm}$) of irradiance followed by 18 min of condensation. The test was performed for 200 h. Taking as reference the solar energy per year in Northern Spain, i.e., 188.28 MJ/m^2 for a wavelength range from 300 to 800 nm, it could be estimated that the test is equivalent to approximately 70 days under environmental conditions.

Chemical resistance tests were performed by immersing the samples in different agents (bleach, olive oil, vinegar, 0.1 M sodium hydroxide, 0.1 M hydrochloric acid). Color properties were monitored further to detect macroscopic changes. After 24 h at room temperature, the samples were removed and dried. Specimens were cleaned using paper soaked with ethanol.

RESULTS AND DISCUSSION

Laser Marking Process

A UV laser was selected for the laser marking process in order to decrease thermal effects associated with marking by an IR laser [20] and to enhance possible photochemical reactions. The different irradiated areas ($1 \text{ cm} \times 1 \text{ cm}$) are shown in Fig. 1. The marks are macroscopically homogeneous, and only when the sample was analyzed under the microscope could the dotted structure resulting from the experimental conditions be observed.

The marks can be optically characterized by the CIELab parameters $L^*a^*b^*$. Coordinate L^* is defined as luminosity and it ranges from $L^* 0$ (black) to $L^* 100$ (white). For black and white materials the a^* and b^* coordinates are 0 or close to 0, so they will not be considered. The evolution of L^* for different

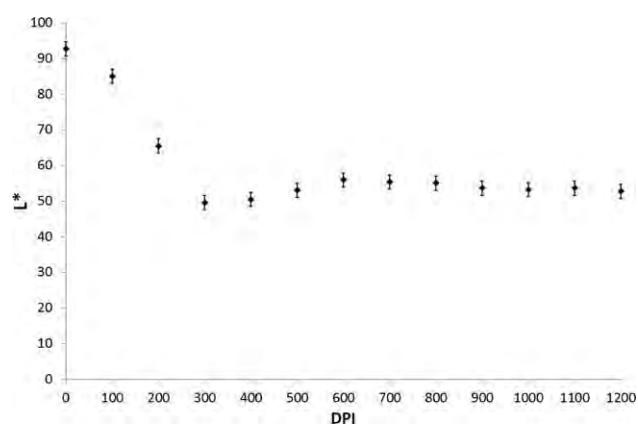


FIG. 2. Luminosity, L^* , coordinate (CIELAB system) for the unmarked (0 DPI) and marked regions as a function of the DPI parameter.

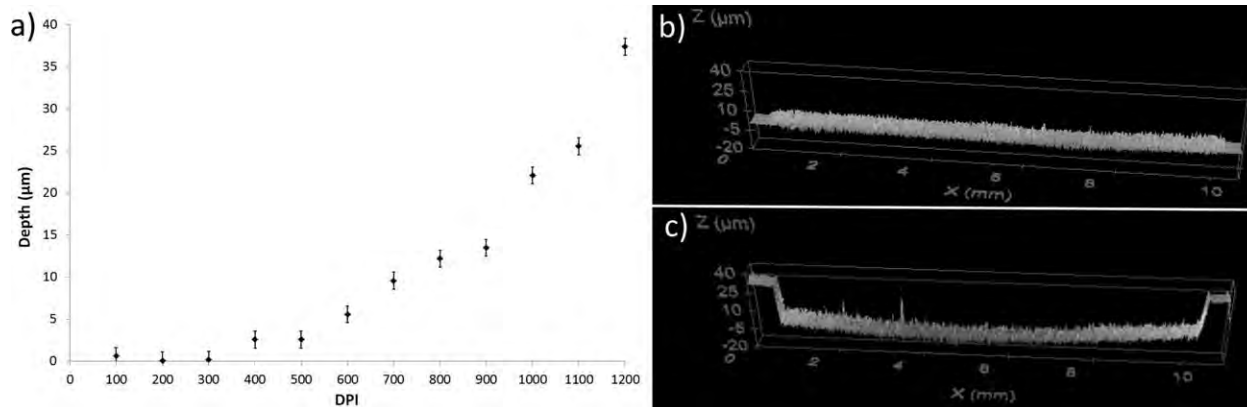


FIG. 3. (a) Mean depth of the marked zone as a function of the DPI parameter, (b) depth profile of a sample marked at 400 DPI, (c) depth profile of a sample marked at 1,200 DPI.

samples marked with different DPI values is represented in Fig. 2. A minimum L^* value is reached at 300 DPI, and it remains approximately constant at higher DPI values (although it increases slightly). The optimum deposited energy on the surface is therefore approximately 1.7 J/cm^2 (calculated from Eq. 1) and this corresponds to 300 DPI. Higher DPI values do not improve the contrast, and in order to select the best mark, low DPI values are preferred to minimize surface damage. It is important to note that for 300 DPI the surface of the polymer is not fully covered by the laser spots (see Supporting Information Figure SI.1), an effect that can be observed microscopically but not macroscopically. Taking this into account, further analysis was conducted on the 400 DPI mark having a more covered area.

Surface and Structural Characterization

The depth of the mark was studied by confocal microscopy and optical microscopy. The evolution of the depth of the marked area measured by confocal microscopy is shown in Fig. 3a. The mean depth is below $5 \mu\text{m}$ for samples marked up to 500 DPI. However, for higher DPIs, the depth increases sharply as a consequence of the engraving produced by laser irradiation. Figure 3b and c represent the depth profile of marks made at 400 DPI and 1,200 DPI, respectively. The quantity of material removed by laser ablation may be roughly associated to the mark depth since the mark area is in all the cases 1 cm^2 . The material began to be clearly ablated at dpi above 500 DPI. Furthermore, laser DPI parameters above 300–400 DPI do not improve the contrast. Consequently, the optimum parameter seems to be around 400 DPI because of the contrast of the marks with minimum ablation and also the process time since a higher DPI value implies a higher processing time.

The cross section was also studied. Samples were first immersed in liquid nitrogen and then fractured. Optical observation of marks made at 400 DPI showed that the color change was not regular and was detected up to $70 \mu\text{m}$ from the surface (see Supporting Information Figure SI.2.a). Optical observation of marks made with 1,200 DPI showed a color change up to $15 \mu\text{m}$ (see Supporting Information Figure SI.2.b), although it should be considered that in this case some material is removed by laser ablation (engraving detected by confocal microscopy).

The surface and the cross section were observed by ESEM. Thus, when the sample marked with 400 DPI was tilted by 10° , several valleys were observed with a depth of ca. $10 \mu\text{m}$ (see Fig. 4). In the sample made with 1,200 DPI, differences along the mark were found (see Supporting Information Figure SI.3). Valleys were observed at both edges; however, at one edge depth measurements were approximately $40 \mu\text{m}$ and at the other edge they were approximately $15 \mu\text{m}$, which is related to the marking direction of the laser and the subsequent accumulated material. In addition, in this sample, an affected region within the marked area was detected with a depth of approximately $7\text{--}10 \mu\text{m}$, see Supporting Information Figure SI.3 green square.

Attenuated total reflectance (ATR)-FTIR was used to characterize the chemical structure of the sample surface. The IR spectra of the marked areas, with different laser parameters, were

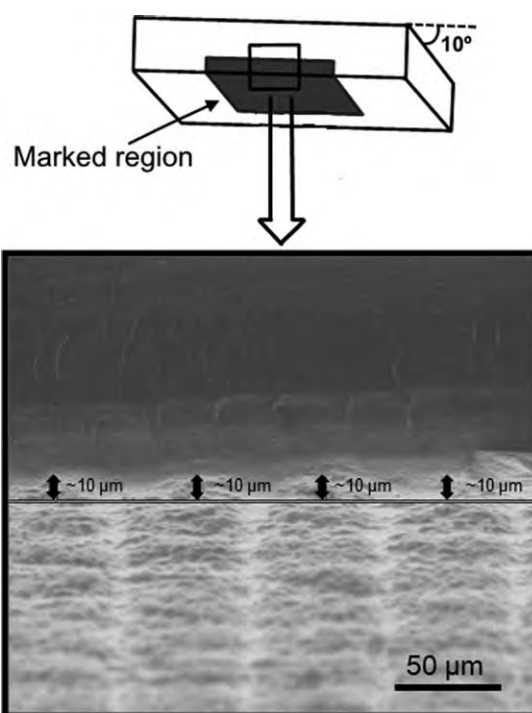


FIG. 4. ESEM image of a sample marked with 400 DPI.

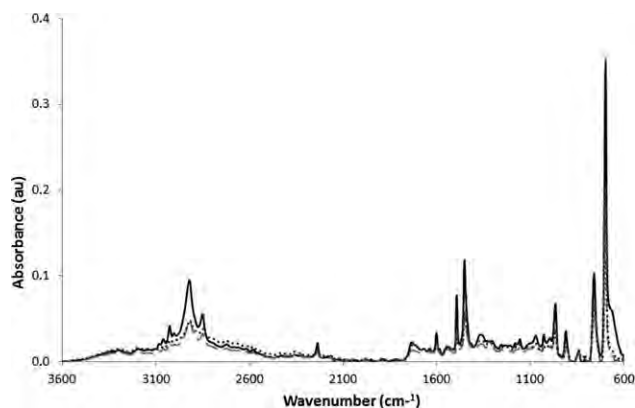


FIG. 5. ATR-FTIR spectra of unmarked ABS and marked samples with different DPI parameters (solid line—unmarked ABS sample, dashed line—400 DPI, dotted line—1,200 DPI).

recorded and compared with those of unmarked regions. The ATR-FTIR spectrum of an unmarked region (continuous line) is shown in Fig. 5. The peaks are consistent with an ABS polymer spectrum. The spectra of a marked sample with 400 DPI (dashed line) and 1,200 DPI (dotted line) are also shown in Fig. 5. In the marked samples, signals corresponding to ABS are also clearly identified with no significant evidence of degradation, which indicates that the UV marking does not have a critical influence on the chemical structure of the plastic material. Significant changes were not observed between samples marked

with the different parameters used for laser marking. In some cases, minor changes (in intensity) can be appreciated depending on the measured area, although this finding can be attributed to a change in the roughness of the marked area. Nevertheless, a shoulder at approximately 600 cm⁻¹ is observed in the unmarked samples and this is related to the rutile form of TiO₂. As can be seen, this shoulder decreases in intensity when the sample is marked with the UV laser, which seems to indicate that this additive is affected by laser irradiation.

TiO₂ is an additive that absorbs UV radiation and under intense UV laser irradiation, a visible change in color can be observed for this additive [25–27]. It has been reported that this change could be associated with the generation of reduced species of titanium [25, 26]. The amount of TiO₂ added to the material can play an important role in the mark quality in terms of significant depth of color change and low reflectivity [21, 28]. TGA was performed in order to determine the inorganic residues of the material. Thermal analyses were reproducible and the final solid residue detected was approximately 6.5 wt%, which can be mainly assigned to the white pigment (see Supporting Information Figure SI.4 for an example). The titanium content was also determined by inductively coupled plasma atomic emission spectroscopy (ICP-OES). The data obtained indicate that the percentage of titanium dioxide in the ABS polymer is approximately 6%.

X-ray photoelectron spectroscopy (XPS) provides information about the elemental composition and electronic state of the elements presented in the material surface. This technique allows

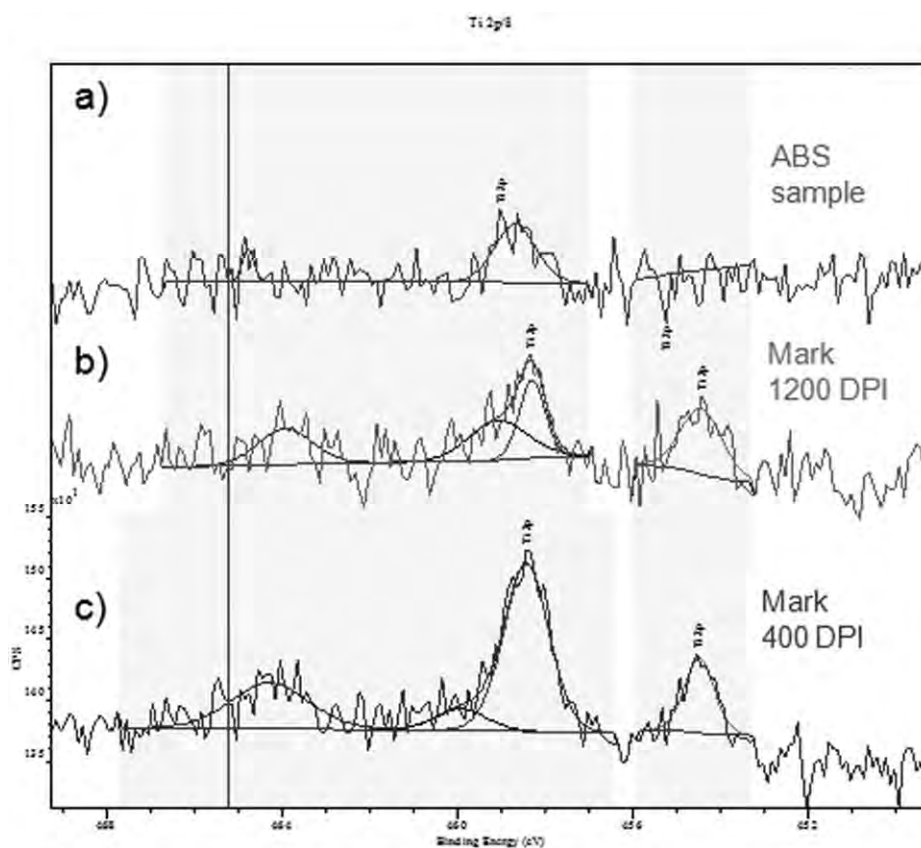


FIG. 6. High-resolution titanium XPS spectra of (a) unmarked ABS sample, (b) sample marked with 1,200 DPI, and (c) sample marked with 400 DPI.

small changes in the superficial irradiated area to be detected. The spectra and detected atomic composition were reproducible within the same area and the elements detected in the surface of the unmarked sample were similar to those detected in marked ABS samples (see Supporting Information Figure SI.5). High-resolution experiments were carefully conducted, first on the original unmarked ABS sample (see Fig. 6a) and also in the marked materials (see Fig. 6b and c) in an effort to understand how laser irradiation influences the Ti composition. In the original unmarked ABS samples, peaks for Ti 2p_{3/2} and Ti 2p_{1/2} were detected at 458.9 and 464.4 eV, respectively, and these correspond to titanium dioxide [29]. In marked samples, other peaks for Ti were observed in addition to those mentioned above at 454.5 eV for 2p_{3/2} and 460.4 eV for 2p_{1/2} and these correspond to a reduced state of titanium (see Fig. 6b and c). According to these data, the presence of reduced titanium in the marked samples seems to be related to photoinduced processes that occur during the laser marking, which affect the pigment included in the white ABS. It can be considered that UV-marking does not essentially affect the chemical structure of the polymer but that the white titanium dioxide pigment is affected.

Resistance Behavior of Laser Marked Regions

Three different tests were performed in order to study the resistance behavior of the laser marked regions and these were a scratch test, a climate test, and resistance to chemical agents. The scratch width made by the Erichsen pen is not dependent on the DPI (see Supporting Information Table SI.1). Furthermore, this width on the laser marked samples is very similar to that measured in pad printing samples, and both are slightly higher than the width of the reference material. The laser marking, therefore, seems to show similar behavior in terms of scratch resistance to the traditional printing techniques.

Furthermore, many plastic materials intended for home, offices, or commercial environments must be tested for resistance to environmental conditions. For instance, photodegradation can cause aesthetic defects or product failures. For this reason, we aimed to check the climate resistance of laser marked materials and evaluate possible changes in color. Marked samples were compared before and after performing the test. At first glance, drastic changes were not observed and the laser marks had a good resistance to the test. However, once the climate tests were completed, yellowing of the ABS plastic samples (unmarked ABS regions) was still not detected but bending, probably because to the condensation cycles, was observed. It is important to note, however, that this effect is associated with the mechanical properties of the bulk material and not to the laser marks. In addition, the L* values measured by spectrophotometry for the unmarked material were lower after the test, i.e., the unmarked sample was slightly darker after performing the test (see Supporting Information Figure SI.6). This effect is probably because to the darkening of the unmarked material and it was more appreciable for the lowest DPI values where the laser affected the polymer to a lesser extent. This result denotes the resistance of laser marks to the simulated climate conditions tested.

Contact with chemical reagents may also lead to modifications in the properties of the laser-marked material. The chemical resistance test was performed by immersion of specimens

into different agents. Five different chemical agents were tested and these were related to common products (bleach, olive oil, vinegar, 0.1 M sodium hydroxide, 0.1 M hydrochloric acid) and color properties were monitored to detect macroscopic changes. Marked samples were compared before and after performing the test (see Supporting Information Table SI.2) and marked changes were not found by direct observation of the samples. The differences in the L* coordinate, before and after performing the test, are less than 1.5 (absolute value) and this corresponds to excellent color tolerance. An exception to this behavior is the sample marked with 1,200 DPI immersed in vinegar, where the differences in L* were approximately 2.0. The laser marks have a good resistance to the chemical agents evaluated.

CONCLUSIONS

Different studies were conducted to evaluate the UV-marking process in white ABS samples. According to the results, the best experimental laser parameters to give marks at approximately 400 DPI provide images with good contrast and the roughness or mark depth properties are in the order of 10 μm. Furthermore, the effect of laser marking on the chemical structure of the irradiated surface was studied. It was found that the UV laser marking did not have a significant influence on the overall chemical structure but the titanium dioxide did appear to be modified under irradiation, as deduced from the presence of reduced Ti by XPS on the marked area. Laser marks also had good scratch resistance, which was similar to that of pad painted marks. Additionally, laser marks have a good resistance to chemical agents and climate tests. Laser aesthetical marking on white polymers in the UV range gives rise to quality marks compared to those obtained with other lasers and this approach could be implemented for industrial purposes.

ACKNOWLEDGMENTS

The authors acknowledge analysis services from CEQMA (Centro de Química y Materiales de Aragón, Spain), the Laboratory of Advanced Microscopy Laboratory (LMA, Zaragoza, Spain), “Instituto de Cerámica y Vidrio” (CSIC, Madrid, Spain), ITA (Technological Institute of Aragon, Spain) and BSH Spain.

ABBREVIATIONS

ABS	Acrylonitrile-butadiene-styrene
ATR-FTIR	Attenuated total reflectance-infrared spectroscopy
DPI	Dots per inch
ESEM	Environmental scanning electron microscope
ICP-OES	Inductively coupled plasma atomic emission spectroscopy
IR	Infrared
Nd:YAG	Neodymium-doped yttrium aluminium garnet
SCI	Specular component included
TGA	Thermogravimetric analysis
UV	Ultraviolet
XPS	X-ray photoelectron spectroscopy

REFERENCES

1. D. Bäuerle, *Laser Processing and Chemistry*, Springer Verlag, Berlin (2011).
2. L. Santo, F. Trovalusci, and J.P. Davim, *Compr. Mater. Process.*, **9**, 243 (2014).
3. Y. Md. Noor, S.C. Tam, L.E.N. Lim, and S. Jana, *J. Mater. Process. Technol.*, **42**, 95 (1994).
4. J. Bosman, *Processes and strategies for solid state Q-switch laser marking of polymers*, PhD Thesis, Velden, Netherland (2007).
5. J.J. Pireaux, R. de Meulemeester, E.M. Roberfroid, C. Grégoire, M. Chtaïb, Y. Novis, J. Riga, and R. Caudano, *Nucl. Instrum. Methods Phys. Res. B*, **105**, 186 (1995).
6. T. Lippert, T. Nakamura, H. Niino, and A. Yabe, *Appl. Surf. Sci.*, **109–110**, 227 (1997).
7. T. Lippert, F. Raimondi, J. Wambach, J. Wei, and A. Wokaun, *Appl. Phys. A*, **69**, S291 (1999).
8. P. Laurens, B. Sadras, F. Decobert, F. Arefi, and J. Amouroux, *Appl. Surf. Sci.*, **138–139**, 93 (1999).
9. T.C. Chang and P.A. Malian, *J. Manufac. Proc.*, **1**, 1 (1999).
10. L.D. Laude, D. Martinez, C. Dicara, F. Hanus, and K. Kolev, *Nucl. Instrum. Methods Phys. Res.*, **185**, 147 (2001).
11. J. Yip, K. Chan, K.M. Sin, and K.S. Lau, *Appl. Surf. Sci.*, **205**, 151 (2003).
12. J. Yip, K. Chan, K.M. Sin, and K.S. Lau, *Polym. Int.*, **53**, 627 (2004).
13. P. Rytlewski, and M. Żenkiewicz, *Appl. Surf. Sci.*, **256**, 857 (2009).
14. E. Sancaktar and H. Lu, *J. Appl. Polym. Sci.*, **99**, 1024 (2006).
15. Y. Feng, Z.Q. Liu, and X.S. Yi, *Appl. Surf. Sci.*, **156**, 177 (2000).
16. L. Urech, T. Lippert, C.R. Phipps, and A. Wokaun, *Appl. Surf. Sci.*, **253**, 6409 (2007).
17. P. Laurens, M. Ould Bouali, F. Meducin, and B. Sadras, *Appl. Surf. Sci.*, **154–155**, 211 (2000).
18. Q. Lu, M. Li, J. Yin, Z. Zhu, and Z. Wang, *J. Appl. Polym. Sci.*, **82**, 2739 (2001).
19. J. Breuer, S. Metev, and G. Sepold, *J. Adhes. Sci. Technol.*, **9**, 351 (1995).
20. G. Ricciardi, M. Cantello, and G.S. Aira, *CIRP Ann.*, **45**, 191 (1996).
21. H.Y. Zheng, D. Rosseinsky, and G.C. Lim, *Appl. Surf. Sci.*, **245**, 191 (2005).
22. A. Zohrevand, A. Ajji, and F. Mighri, *Polym. Eng. Sci.*, **54**, 874 (2014).
23. F. Li, S. Zhou, G. Gu, and L. Wu, *Polym. Eng. Sci.*, **46**, 1402 (2006).
24. J. Schneider, M. Matsuoka, M. Takeuchi, J. Zhang, Y. Horiuchi, M. Anpo, and D.W. Bahnemann, *Chem. Rev.*, **114**, 9919 (2014).
25. S.K. Lee, P.K.J. Robertson, A. Mills, D. McStayd, N. Elliott, and D. McPhail, *Appl. Catal. B Environ.*, **44**, 173 (2003).
26. T. Le Mercier, M. Quarton, M.-F. Fontaine, C.F. Hague, and J.-M. Mariot, *J. Appl. Phys.*, **76**, 3341 (1994).
27. H.Y. Zheng, H.X. Qian, and W. Zhou, *Appl. Surf. Sci.*, **254**, 2174 (2008).
28. L.D. Laude, N. Boutarek, and K. Kolev, *Nucl. Instrum. Methods*, **105**, 254 (1995).
29. R. Yao, R. Wu, and G. Zhai, *Polym. Eng. Sci.*, **55**, 735 (2015).